Synthesis of High-Molecular-Weight Bifunctional Additives with both Flame Retardant Properties and Antistatic Properties via ATRP

Shaobo Dong,* Yazhen Wang,* Tianyu Lan, Jianxin Wang, Liwu Zu, Tianyuan Xiao, Yonghui Yang, and Jun Wang

ACCESS | Metrics & More | Article Recommendations

ABSTRACT: Polystyrene (PS) is widely used in our daily life, but it is flammable and produces a large number of toxic gases and high-temperature flue gases in the combustion process, which limit its application. Improving the flame retardancy of PS has become an urgent problem to be solved. In addition, in view of the disadvantage that small-molecule flame retardants can easily migrate from polymers during use, which leads to the gradual reduction of the flame retardant effect or even loss of flame retardant performance, and the outstanding advantages of ATRP technology in polymer structure design and function customization, we used ATRP technology to synthesize the high-molecular-weight bifunctional additive PFAA-DOPO-*b*-PDEAEMA, which has flame retardant properties and antistatic properties. The chemical structure and molecular weight of PFAA-DOPO-*b*-PDEAEMA were characterized by FTIR, ^{1}H NMR, GPC, and XPS. When the addition of PFAA-DOPO-*b*-PDEAEMA was 15 wt %, the limiting oxygen index (LOI) of polystyrene composites was 28.4%, which was 53.51% higher than that of pure polystyrene, the peak of the heat release rate (pHRR) was 37.61% lower than that of pure polystyrene, UL-94 reached V-0 grade, and the flame retardant index (FRI) was 2.98. In addition, when the PFAA-DOPO-*b*-PDEEMA content is 15 wt %, the surface resistivity and volume resistivity of polystyrene composites are 2 orders of magnitude lower than those of polystyrene. This research work provides a reference for the design of bifunctional and even multifunctional polymers.
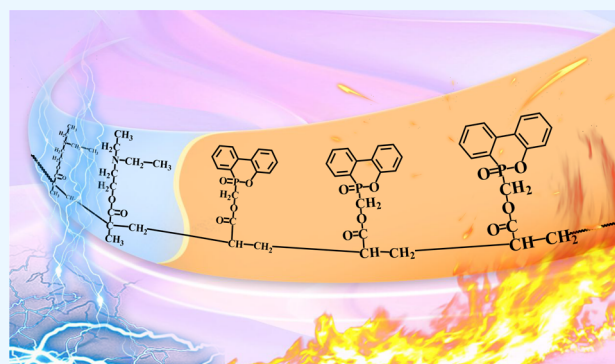
1. INTRODUCTION

With the application of polymer materials becoming more and more widespread, fire caused by the flammability of polymer materials has posed a threat to the safety of people's lives and property, and the flame retardant problem of polymer materials needs to be solved urgently.[1] In the final analysis, the methods to improve the flame retardancy of polymer materials can be divided into two types: materials design and materials processing. In general, flame retardants are added to polymer materials to improve the flame retardancy of polymer materials.[2] The flame retardant systems mainly include mineral flame retardants,[3−6] halogen flame retardants, nitrogen flame retardants,[7−9] silicone flame retardants,[10−12] bio-based flame retardants[13−16] and phosphorus flame retardants.[17−23] Among them, a mineral flame retardant needs to be added in a large amount to achieve a flame retardant effect, which will have a certain influence on other properties of materials and halogen flame retardants are prohibited in many fields because of their high toxicity. The application of nitrogen flame retardants is limited due to their low thermal stability. A phosphorus flame retardant is considered as the best substitute for a halogen flame retardant because of its nontoxicity.[1,13] Jiang et al.

synthesized the DOPO-based macromolecular flame retardant DOPONH$_2$-S containing P/N/S for flame retardancy of epoxy resin. When the mass percentage of DOPONH$_2$-S is 6.75 wt %, the LOI of the epoxy resin composite is 30.5% and UL-94 reaches the grade V-0. At the same time, the impact strength of the epoxy resin composite is improved by 62.5%, with good toughness and no damage to T_g.[18] Zhao et al. synthesized an efficient modifier for MXD6 by combining a DOPO derivative (DT) and the nucleating agent Bruggolen P22. When 11.0 wt % DT and 0.1 wt % P22 were added, the crystallinity of MXD6 increased by 60%, LOI increased by 26.52%, and the FRI was 1.65.[24] Zhao et al. synthesized a reactive flame retardant (DTP) containing triazole, phosphaphenanthrene, and hydroxy groups; although the addition of DTP weakens the stability of epoxy thermosets, it decreases the degradation rate

and increases the char yield at 750 °C. With the addition of 6 wt % DTP (P content: 0.5 wt %), the LOI value of the epoxy resin composite was 31.42% and obtained a V-0 rating in a UL-94 test.[25] Zhang et al. adopted a 9,10-dihydro-9-oxa-10-phosphaphenanthrene-10-oxide derivative (DiDOPO) with a conjugated structure as a new conjugated flame retardant. Polypropylene (PP)/DiDOPO conjugated flame retardant composites were prepared by melt extrusion with a twin-screw extruder. It is said in this paper that DiDOPO can significantly improve the flame retardant effect of PP. When the content of DiDOPO in conjugated structure was 16 wt %, the LOI value of polypropylene composites was 24%, reaching V-0 grade, and the composites might have low conductivity and charge mobility. In addition, according to the data provided in this paper, the FRI value at this time was 0.80.[26] Yang et al. synthesized the multifunctional flame retardant EAD with a conjugated structure by an addition reaction of P–H of DOPO and the alkynyl group of 4-ethynylaniline (EA). When 2 wt % EAD was added to the epoxy resin, the phosphorus loading was only 0.186 wt %, which could effectively improve the flame retardancy of the epoxy resin and LOI increased by 31% and UL-94 reached V-0 grade.[27] To sum up, DOPO is often used as a basic raw material to synthesize phosphorus flame retardants with high molecular weight, and these DOPO-based flame retardants have obvious flame retardant effects. However, these DOPO-based flame retardants with large molecular weight are still small-molecule flame retardants, and their structures and functions cannot be customized.

In recent years, there have been more and more studies on bifunctional and multifunctional additives with flame retardancy and other functions.[28−45] Gao et al. prepared PS/silicon-wrapped ammonium polyphosphate/multiwall carbon nanotube (PS/SiAPP/MWCNT) composites with a segregated structure via the methods of ball milling and hot pressing. The PS/SiAPP/MWCNT hybrid material was a satisfactory electromagnetic interference shielding material with excellent flame retardancy for electronic equipment.[46] In addition, Gao et al. also deposited high-efficiency cetyltrimethylammonium bromide/multiwall carbon nanotubes@two-dimensional titanium carbide (C-MWCNT@Ti$_3$C$_2$T$_x$) on PS to prepare PS@C-MWCNT@Ti$_3$C$_2$T$_x$ composites. SiAPP-NH$_2$@Ti$_3$C$_2$T$_x$ was prepared by coating ammonium polyphosphate (APP-NH$_2$) with γ-propyltrimethoxysilane and Ti$_3$C$_2$T$_x$. Polystyrene composites with good flame retardancy and electromagnetic shielding properties were obtained by adding SiAPP-NH$_2$@Ti$_3$C$_2$T$_x$ to prepare PS@C-MWCNT@Ti$_3$C$_2$T$_x$.[47] Li et al. prepared an P–N–Si integrated flame retardant (DGO) by modifying DOPO with γ-aminopropyltriethoxysilane and graphene oxide through mild Mannich and silanization reactions and then made DGO and phenolic resin into a coating material to obtain a multifunctional flame retardant for building insulation.[48] Yuan et al. took a lotus leaf as a design inspiration and prepared a hydrophobic porous metal−organic framework (S-FeMOF) that significantly improved the flame retardancy of PS on the basis of their original work, which provided inspiration for the design of a hydrophobic structure and enlightenment for the preparation of multifunctional materials.[49] Zhu et al. synthesized the multifunctional additives 5,10,15,20-tetra(4-bromophenyl)porphyrin and zinc 5,10,15,20-tetra(4-bromophenyl) orphyrin to improve the mechanical properties, ultraviolet resistance, thermal stability, and fire safety of polystyrene.[50] It can be seen that the research

on developing bifunctional and even multifunctional additives with flame retardancy is increasing.

Controlled radical polymerization techniques, including atom transfer radical polymerization (ATRP) and reversible addition−fragmentation chain-transfer (RAFT) polymerization, have been developed in the field of precision polymer chemistry.[51] ATRP is one of the most important living/controlled free radical polymerizations. Compared with the traditional free radical polymerization, ATRP has the characteristics of a controllable molecular weight of the polymer and a narrow molecular weight distribution, and ATRP is usually used in polymer molecular design to customize the molecular structure and function of polymers.[51−59] Cao et al. successfully copolymerized various vinyl monomers, including acrylate, styrene, acrylonitrile, and acrylamide, with α-haloacrylate by the ATRP technology, which realized chain growth, and a high monomer conversion rate and produced well-defined branched polymers with tunable degrees of branching.[52] Tamura et al. first synthesized the macromonomer poly(methyl methacrylate) (PMMA) by the ATRP technology and then prepared a PMMA bottle brush polymer by ring-opening metathesis polymerization then used the PMMA bottle brush polymer to effectively control and eliminate the orientation birefringence of the optical polymer PMMA.[60] It can be seen that ATRP has unique advantages in polymer structure design and function predetermination.

Electroconductive PS composites with ideal flame-retardant properties are considered as potential electromagnetic interference (EMI) shielding materials.[46] For the phosphorus-containing flame retardant DOPO and its derivatives usually are designed to possess double bonds for polymerization,[61] and some studies have shown that the amino groups are protonated and hydrophilic.[62] Therefore, we expect to use the ATRP technology to achieve the combination of DOPO and DEAEMA properties and prepare a bifunctional high-molecular-weight additive with flame retardancy and a certain conductivity with a controllable structure. In addition, many years of experience have confirmed that screw extruders are better machines for the preparation of materials with a heterogeneous composition. This is mainly due to the higher shear stress generated on materials and a more efficient heat and mass transfer of screw extruders compared to piston extruders. Melt compounding via screw extrusion is an efficient technique for the preparation of novel polymer blends and composites.[2] Therefore, we chose a twin-screw extruder to mix the composites fully and uniformly before sample preparation.

2. MATERIALS AND METHODS

2.1. Materials. 9,10-Dihydro-9-oxa-10-phosphaphenanthrene 10-oxide (DOPO, 97%, AR), anhydrous ethanol (99.5%, AR), formaldehyde aqueous solution (FA, 37%, AR), triethylamine (TEA, 99%, AR), dichloromethane (DCM, 99.5%, AR), acryloyl chloride (AC, 96%, stabilized with 200 ppm of 4-methoxyphenol, AR), N,N-dimethylformamide (DMF, 99.5%, AR), ethyl α-bromoisobutyrate (EBiB, 98%, AR), N,N,N′,N″,N″-pentamethyldiethylenetriamine (PMDETA, 99%, AR), acetic acid (99.5%, AR), 2-(diethylamino)ethyl methacrylate (DEAEMA, 99%, AR), and cuprous bromide (CuBr, AR) were purchased from Shanghai Aladdin Biochemical Technology Co., Ltd. Polystyrene (158 K) was purchased from BASF-YPC Co., Ltd. These reagents were used

Scheme 1. Synthesis Route for FA-DOPO, FAA-DOPO, PFAA-DOPO-Br, and PFAA-DOPO-b-PDEAEMA
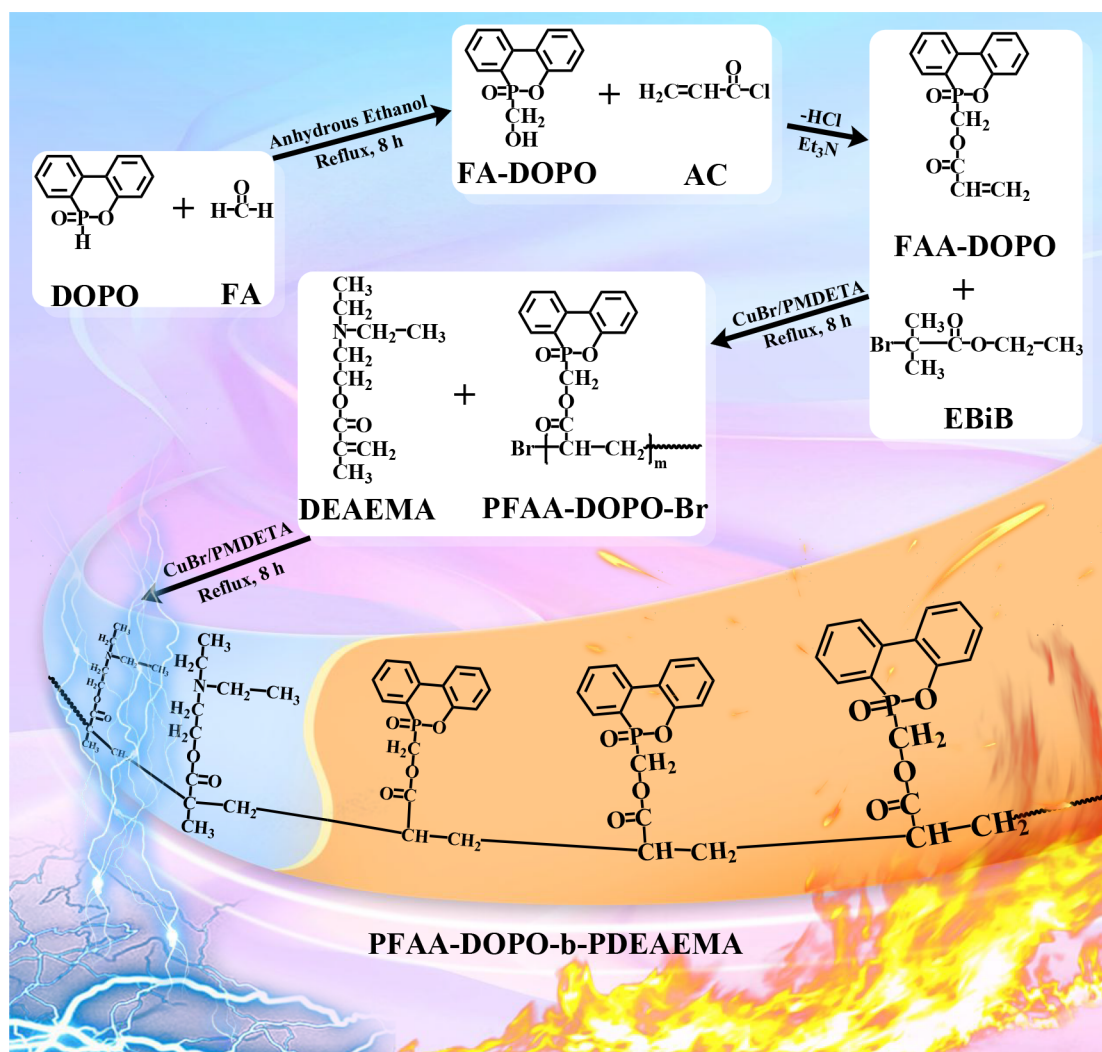
as received without further purification, except that CuBr was purified with acetic acid before use.

2.2. Synthesis of 6-(Hydroxymethyl)dibenzo[c,e][1,2]-oxaphosphinine 6-oxide (FA-DOPO). Referring to Wang's literature method,[61] the method[63] in Zhou's study was improved, and FA-DOPO was synthesized by a one-step feeding method. The synthetic procedures of FA-DOPO are illustrated in Scheme 1. DOPO (89.14 g, 0.4 mol) and 37% FA aqueous solution (40.58 g, 0.5 mol) were dissolved in 250 mL of anhydrous ethanol in a four-necked round-bottom flask equipped with a magnetic stirring rotor, a condenser tube, a thermometer, and a nitrogen protection device. Then the mixture was heated to 60 °C with stirring until the mixed solution became a uniform transparent solution; then the reaction temperature was increased to 95 °C and the solution refluxed for 8 h. After cooling to room temperature and standing overnight, the precipitated white powder was collected by filtration, washed several times with anhydrous ethanol, and dried under vacuum at 40 °C. Yield: 90%. ^{1}H NMR (600 MHz, CDCl$_3$, ppm): δ 8.03 (dd, J = 8.1, 4.8 Hz, 1H), 8.01−7.94 (m, 2H), 7.75 (t, J = 7.7 Hz, 1H), 7.56 (ddd, J = 7.9, 7.0, 3.2 Hz, 1H), 7.42−7.38 (m, 1H), 7.28 (dd, J = 9.0, 1.4 Hz, 2H), 4.31−4.19 (m, 2H), 2.37 (s, 1H). FTIR (KBr, cm^{-1}): 3316 (CH$_2$−OH), 2930 (−CH$_2$−), 1585 (P−Ph),

1208 (P=O), 1120, 760 (P−O−Ph). The band at 2440 cm^{-1} belonging to a P−H bond disappeared.

2.3. Synthesis of (6-Oxidodibenzo[c,e][1,2]-oxaphosphinin-6-yl)methyl acrylate (FAA-DOPO). Referring to Wang's literature method,[61] the synthetic procedures of FAA-DOPO are illustrated in Scheme 1. The detailed synthesis processes are shown as follows. FA-DOPO (49.24 g, 0.2 mol) and TEA (20.44 g, 0.2 mol) were dissolved in 100 mL of DCM in a four-necked round-bottom flask equipped with a magnetic stirring rotor, a condenser tube, a thermometer, a nitrogen protection device, and a constant-pressure dropping funnel. AC (18.86 g, 0.20 mol) in 50 mL of DCM was added dropwise at −5 to 0 °C over 6 h with the constant-pressure dropping funnel. The mixture then was heated to room temperature and stirred for 24 h. Subsequently, the precipitated triethylamine hydrochloride was removed by filtering, and the filtrate was rotary evaporated to remove the solvent under reduced pressure. The residue was washed with DCM, the rotary evaporation step was repeated, and the product was dried under vacuum at 40 °C; an orange-yellow viscous product was obtained. Yield: 80%. ^{1}H NMR (600 MHz, CDCl$_3$, ppm): δ 8.04−7.99 (m, 1H), 7.99−7.90 (m, 2H), 7.75 (ddt, J = 8.4, 7.3, 1.2 Hz, 1H), 7.58−7.52 (m, 1H), 7.38 (ddt, J = 8.9, 7.7, 1.4 Hz, 1H), 7.26−7.22 (m, 2H), 6.01 (dd, J = 17.3, 1.3 Hz, 1H),

5.78 (dd, J = 17.3, 10.5 Hz, 1H), 5.66 (dd, J = 10.5, 1.3 Hz, 1H), 4.87−4.64 (m, 2H). FTIR (KBr, cm^{-1}): 2930 (−CH$_2$−), 1740 (C=O), 1625 (C=C), 1585 (P−Ph), 1208 (P=O), 1120, 760 (P−O−Ph). The band at 3316 cm^{-1} belonging to the CH$_2$−OH bond disappeared.

2.4. Synthesis of Macroinitiator PFAA-DOPO-Br via ATRP.

PFAA-DOPO-Br was synthesized using the ATRP technique as follows; the synthetic procedures of PFAA-DOPO-Br are illustrated in Scheme 1. FAA-DOPO (6.005 g, 0.02 mol), EBiB (0.039 g, 0.0002 mol), CuBr (0.0287 g, 0.0002 mol), and PMDETA (0.104 g, 0.0006 mol) were dissolved in 100 mL of DMF in a four-necked round-bottom flask equipped with a magnetic stirring rotor, a condenser tube, a thermometer, and a gas inlet/outlet. The reaction mixture was deaerated by nitrogen gas for some minutes, and then the reaction temperature was raised to 130 °C and the mixture refluxed for 9 h. After the mixture was cooled to room temperature, the precipitated light yellow powder was collected by filtration, washed several times with anhydrous ethanol, and dried under vacuum at 40 °C. ^{1}H NMR (600 MHz, CDCl$_3$): δ 7.86 (s, 3H), 7.57 (s, 1H), 7.37 (s, 1H), 7.23(s, 1H), 7.11 (s, 2H), 4.53 (s, 2H), 3.42(s, 1H), 3.13−2.66 (m, 2H). FTIR (KBr, cm^{-1}): 2930 (−CH$_2$−),1740 (C=O), 1585 (P−Ph), 1208 (P=O), 1120, 760 (P−O−Ph). The band at 1625 cm^{-1} belonging to the C=C bond disappeared.

2.5. Synthesis of PFAA-DOPO-b-PDEAEMA via ATRP Using PFAA-DOPO-Br Initiator.

PFAA-DOPO-b-PDEAE-MA was synthesized using the ATRP technique as follows; the synthetic procedures of PFAA-DOPO-b-PDEAEMA are illustrated in Scheme 1. DEAEMA (9.3566 g, 0.05 mol), PFAA-DOPO-Br (13.26g, 0.0005 mol), CuBr (0.0717 g, 0.0005 mol), and PMDETA (0.2626g, 0.0015 mol) were dissolved in 300 mL of DMF in a four-necked round-bottom flask equipped with a magnetic stirring rotor, a condenser tube, a thermometer, and a gas inlet/outlet. The reaction mixture was deaerated by nitrogen gas for some minutes, and then the reaction temperature was raised to 130 °C and the mixture refluxed for 9 h. After the mixture was cooled to room temperature, the precipitated yellow powder was collected by filtration, washed several times with anhydrous ethanol, and dried under vacuum at 40 °C. ^{1}H NMR (600 MHz, CDCl$_3$): δ 8.05−7.18 (m, 8H), 4.53 (s, 9H), 3.42 (s, 1H), 3.13−2.66 (m, 2H), 2.16 (s,7H). FTIR (KBr, cm^{-1}): 2930 (−CH$_2$−), 2870 (−CH$_3$), 1740 (C=O), 1585 (P−Ph), 1208 (P=O), 1120, 760 (P−O−Ph).

2.6. Preparation of PFAA-DOPO-b-PDEAEMA/Polystyrene Test Splines.

PFAA-DOPO-b-PDEAEMA and polystyrene were mixed with a GRH-10 high speed mixer according to the mass ratios of 0%, 2%, 4%, 6%, 8%, 10% and 15%, respectively, extruded by a SHJ-20B double-screw extruder, and pelletized by a JDIA pelletizer, and the test samples were prepared by a FH-100 injection molding machine.

2.7. Characterization.

^{1}H NMR spectra were recorded with a Bruker AVANCENMR instrument operating at 600 MHz for ^{1}H at room temperature, using CDCl$_3$ (^{1}H, 7.26 ppm) as a solvent with the internal standard TMS (^{1}H, 0.00 ppm).

The Fourier transform infrared (FTIR) spectra were recorded with a PerkinElmer Spectrum One B spectrometer using KBr pellets. Spectra in the range of 4500−450 cm^{-1} were obtained by 32 scans at a resolution of 4 cm^{-1}.

The X-ray photoelectron spectra (XPS) were recorded with a Thermo ESCALAB250Xi spectrometer using Al Kα excition radiation ($h\nu$ −5000 eV).

The number-averaged molar mass ($\bar{M}_n$) and polydispersity index (PDI) were determined with a Wyatt GPC/SEC-MALS instrument equipped with a DAWN 8 laser light scattering detector and an Optilab T-Rex refractive index detector, using DMF (0.5 mL/min) with 0.1 M LiBr as the mobile phase at 50 °C, and polystyrene standards with narrow distributions were used for calibration.

The limiting oxygen index (LOI) measurement was carried out with a JF-3 oxygen index measurement instrument according to the GB/T2406.2-2009 testing procedure with a sample size of 100 mm × 10 mm × 4 mm (length × width × thickness).

Cone calorimeter (CC) tests were carried out with an FTT Cone calorimeter according to ISO 5660 with a heat flux of 50 kW m^{-2}. The experiments were terminated after the flame stopped for 100 s. The sample size was 100 mm × 100 mm × 3 mm (length × width × thickness).

Vertical burning tests (UL-94) tests were carried out with a M607 UL-94 instrument according to GB/T 2408-2021. The dimension of specimens was 125.0 mm × 13.0 mm × 3.0 mm (length × width × thickness).

Vahabi proposed a dimensionless measure to quantify the flame retardancy of thermoplastic polymer matrix composites by measuring the peak of the heat release rate (pHRR), total heat release (THR), and time to ignition (TTI) based on cone calorimetry, and defined it as the flame retardant index (FRI). The FRI was defined as the ratio THR × $\left(\frac{\text{pHRR}}{\text{TTI}}\right)$ between the neat polymer and the corresponding thermoplastic composite containing only one flame retardant additive, and the FRI can be categorized into FRI < 1, 1 < FRI < 10, and 10 < FRI < 100, corresponding to the flame retardancy performance symbolized as "poor", "good" and "excellent", respectively.[1,24,64−66]

flame retardancy index (FRI)

$$= \frac{\left[\text{THR} \times \left(\frac{\text{pHRR}}{\text{TTI}}\right)\right]_{\text{neat polymer}}}{\left[\text{THR} \times \left(\frac{\text{pHRR}}{\text{TTI}}\right)\right]_{\text{composite}}} \tag{1}$$

The surface resistivity (ρ_s) and volume resistivity (ρ_v) of composite materials were measured by a PC68 high resistivity meter made by Shanghai No.6 Electric Meter Factory, which was used to characterize the antistatic properties of the materials. A, ρ_v, and ρ_s are calculated using eqs 2−4, respectively:

$$A = \frac{\pi}{4}(d_1 + g)^2 \tag{2}$$

$$\rho_v = R_v \frac{A}{h} \tag{3}$$

$$\rho_s = R_s \frac{P}{g} \tag{4}$$

In these formulas, A is the effective area of the protected electrode in m^2, d_1 is the diameter of the protected electrode in m; g is the gap between measuring electrodes in m, ρ_v is the volume resistivity in Ω m; R_v is the volumetric resistance in Ω; h is the thickness of the sample in m, ρ_s is the surface resistivity
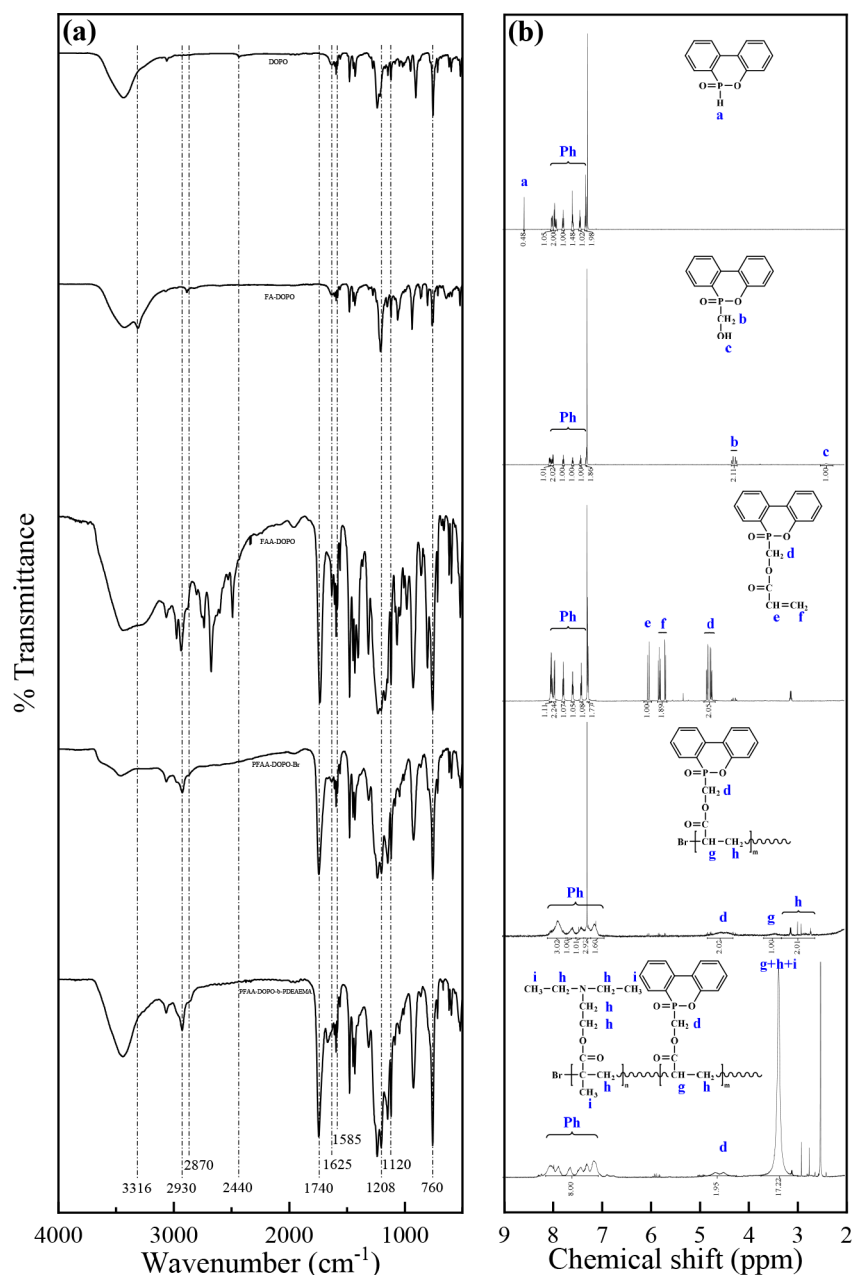
Figure 1. (a) FTIR spectra and (b) ^{1}H NMR spectra of DOPO, FA-DOPO, FAA-DOPO, PFAA-DOPO-Br, and PFAA-DOPO-b-PDEAEMA.

in Ω m, R_s is the surface resistance in Ω, and P is the effective perimeter of the protected electrode in m.

3. RESULTS AND DISCUSSION

3.1. Structure Characterization of PFAA-DOPO-b-PDEAEMA. *3.1.1. FTIR Analysis.* The FTIR spectrum of PFAA-DOPO-b-PDEAEMA is shown in Figure 1a. For convenience of comparison, FTIR spectra of DOPO, FA-DOPO, FAA-DOPO, and PFAA-DOPO-Br are also provided in Figure 1a.

As far as the FTIR spectrum of FA-DOPO is concerned, after the addition reaction between DOPO and FA, the absorption peak at 2440 cm^{-1} for the P–H stretching vibration in DOPO disappeared, while a new absorption peak at 3316 cm^{-1} for the C–OH stretching vibration appeared. The absorption peaks at 1585 cm^{-1} (P–Ph), 1208 cm^{-1} (P=O),

and 1120 and 760 cm^{-1} (P–O–Ph) were assigned to the cyclic DOPO structure, which was well maintained.

For FAA-DOPO, when the substitution reaction between FA-DOPO and AC occurred, the peak at 3316 cm^{-1} for the C–OH stretching vibration disappeared, and new peaks at 1740 cm^{-1} for C=O and 1625 cm^{-1} for the C=C stretching vibration can be observed clearly, which demonstrated the presence of an acrylate group in FAA-DOPO. Besides these, the other characteristic absorption peaks that belonged to the cyclic DOPO structure were still well maintained in FAA-DOPO.

When the macroinitiator PFAA-DOPO-Br was prepared by ATRP polymerization with FAA-DOPO as the monomer, the band at 1625 cm^{-1} for the C=C stretching vibration in FAA-DOPO disappeared and the other characteristic absorption peaks that belonged to the FAA-DOPO structure were still well maintained in PFAA-DOPO-Br.

For the block copolymer PFAA-DOPO-b-PDEAEMA, it can be seen that the functional groups of PFAA-DOPO-b-PDEAEMA and PFAA-DOPO-Br have almost the same chemical structures as shown in Scheme 1, and according to Dong[67] and Lu,[68] the position of the N−C chemical bond of the tertiary amine in PFAA-DOPO-b-PDEAEMA is difficult to distinguish, as shown in Figure 1a; the positions of the characteristic functional groups in the FTIR spectra of PFAA-DOPO-b-PDEAEMA and PFAA-DOPO-Br are almost the same, but the peak intensity of the characteristic functional groups is increased.

3.1.2. ^{1}H NMR Analysis. A ^{1}H NMR spectral comparison of DOPO, FA-DOPO, FAA-DOPO, PFAA-DOPO-Br, and PFAA-DOPO-b-PDEAEMA is provided in Figure 1b. As far as the ^{1}H NMR spectrum of FA-DOPO is concerned, the signal of P−*H*(a) in 8.56 ppm disappeared. The signals of the Ph−*H* proton were observed in the range 8.03−7.28 ppm. The chemical shifts of the characteristic protons −C(OH)−*H*(b) and C−O*H*(c) were found at 4.31−4.19 and 2.37 ppm, respectively, confirming the expected structure of FA-DOPO.

As compared to FA-DOPO, the characteristic shifts of C−O*H*(c) completely disappeared in FAA-DOPO, and the −C*H*=C*H₂*(e,f) protons gave rise to signals in the range of 6.01−5.66 ppm, which demonstrated the existence of an acrylate group. Additionally, the ^{1}H NMR spectra of −C*H₂*(b)− in FA-DOPO and −C*H₂*(d)− in FAA-DOPO showed signals at 4.31−4.19 and 4.87−4.64 ppm, respectively, because of the different chemical environment.

As compared to FAA-DOPO, the characteristic shifts of −C*H*=C*H₂*(e,f) completely disappeared in PFAA-DOPO-Br, and the −C*H*(g)− and −C*H₂*(h)− protons gave rise to signals at 3.42 and 3.13−2.66 ppm, respectively. Additionally, the ^{1}H NMR spectra of Ph−*H* and −C*H₂*(d)− in PFAA-DOPO-Br showed signals at 7.86−7.11 and 4.53 ppm, respectively. Furthermore, these ^{1}H NMR peaks present hill-like peaks that polymers should have.

As compared to PFAA-DOPO-Br, the characteristic shifts of Ph−*H* and −C*H₂*(d)− are almost unchanged, but the relative proportion of the number of protons has changed. Additionally, the ^{1}H NMR spectra of−C*H*(g)−, −C*H₂*(h)−, and −C*H₃*(i) in PFAA-DOPO-b-PDEAEMA showed signals at 3.36 ppm. Furthermore, these ^{1}H NMR peaks present hill-like peaks that polymers should have.

In addition, we will use GPC and XPS to further characterize the successful synthesis of PFAA-DOPO-b-PDEAEMA.

3.1.3. GPC Analysis. The GPC trace of PFAA-DOPO-b-PDEAEMA is shown in Figure 2. For better comparison, the GPC trace of the corresponding macroinitiator PFAA-DOPO-Br is also shown in Figure 2. The number-average molecular weights of PFAA-DOPO-Br and PFAA-DOPO-b-PDEAEMA were 26520 and 38700, respectively, and the PDIs of PFAA-DOPO-Br and PFAA-DOPO-b-PDEAEMA were 1.062 and 1.063, respectively. The number of structural units in PFAA-DOPO-Br and PFAA-DOPO-b-PDEAEMA was calculated according to the GPC test results and the molecular weight of each structural unit in the polymer. According to the calculated results, PFAA-DOPO-Br and PFAA-DOPO-b-PDEAEMA were named PFAA-DOPO$_{88}$-Br and PFAA-DOPO$_{88}$-b-PDEAEMA$_{66}$, respectively. Furthermore, the ratio of proton numbers in the polymer structure calculated by GPC measurement is consistent with the corresponding proton integral ratio in ^{1}H NMR spectra.
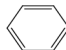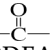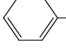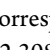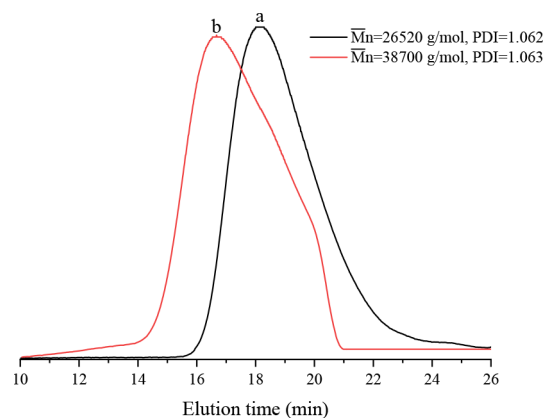

Figure 2. GPC traces of the macroinitiator PFAA-DOPO-Br (a) and the corresponding block copolymer PFAA-DOPO-b-PDEAEMA (b).

3.1.4. XPS Analysis. XPS spectra of PFAA-DOPO-b-PDEAEMA are shown in Figure 3. For a better analysis, the electron binding energy data in the peak fitting diagram of C 1s, O 1s, N 1s, and P 2p in Figure 3 are mapped to the characteristic functional groups of PFAA-DOPO-b-PDEAEMA, and this correspondence is given in Table 1.[69] The chemical environment of O in the molecular structure of PFAA-DOPO-b-PDEAEMA is relatively simple, and according to the above GPC analysis, the numbers of −P−O− bonds, −P=O bonds, −C−O− bonds, ⬡−O− bonds, and —C(O)— bonds in the molecular structure of PFAA-DOPO-b-PDEAEMA are 88, 88, 154, 88, and 154, respectively. Therefore, in the fitting data of O 1s, the fitting peak area corresponding to −P−O− bonds and −P=O bonds, the sums of the fitting peak area corresponding to −C−O− bonds and ⬡−O− bonds and the fitting peak area percentages corresponding to —C(O)— bonds should be 15.385%, 15.385%, 42.308%, and 26.922%, respectively, which is consistent with the peak fitting data of O 1s in Table 1. In addition, in C 1s fitting data, the peak area corresponding to each fitting curve is slightly different from the corresponding functional group percentage in PFAA-DOPO-b-PDEAEMA, but the overall coincidence is very high. The results of XPS analysis were consistent with those of ^{1}H NMR and GPC. According to the above FTIR, ^{1}H NMR, GPC, and XPS analysis results, PFAA-DOPO$_{88}$-b-PDEAEMA$_{66}$ was successfully synthesized by ATRP.

3.2. Flame Retardancy of PFAA-DOPO-b-PDEAEMA. In order to characterize the flame retardancy of PFAA-DOPO-b-PDEAEMA, PFAA-DOPO-b-PDEAEMA was added with polystyrene in different proportions to form test splines. Figure 4 shows the heat release rate (HRR) curve of the samples, and some detailed data, such as LOI, HRC, pHRR, THR, and T_p, are given in Table 2.

According to the LOI data in Table 2, the LOI of the composites showed an upward trend with an increase in the addition of PFAA-DOPO-*b*-PDEAEMA in polystyrene; when the addition of PFAA-DOPO-*b*-PDEAEMA was 15 wt %, the LOI value of the composites increased by 53.51% compared with that of pure polystyrene. As also shown in Figure 4, the HRR value of the composites is significantly lower than that of pure polystyrene. According to the CC data in Table 2, with the increase of PFAA-DOPO-*b*-PDEAEMA content in
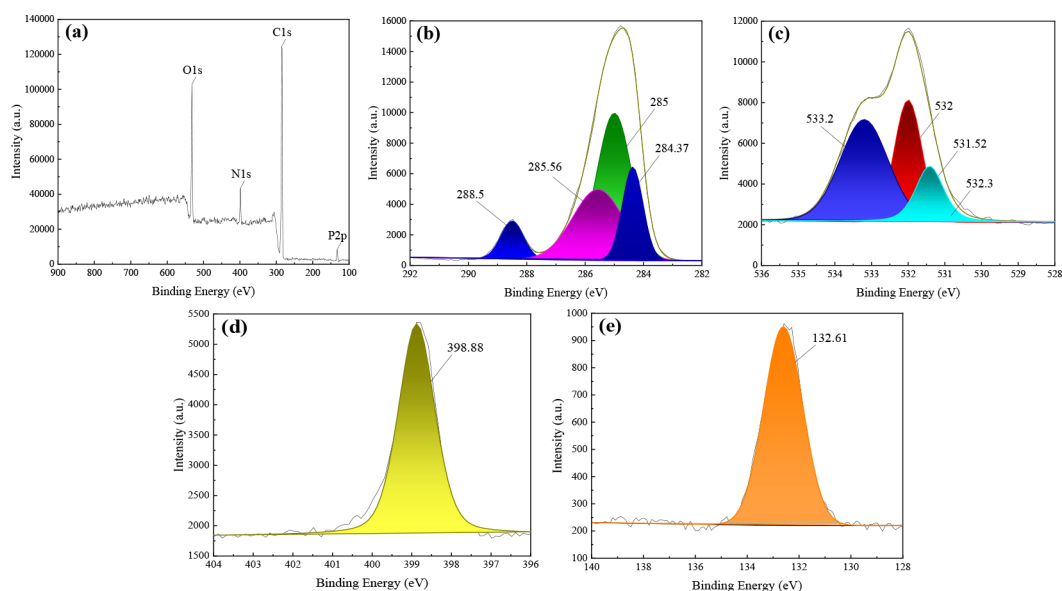
Figure 3. XPS spectra of PFAA-DOPO-b-PDEAEMA: (a) wide-scan spectra of PFAA-DOPO-b-PDEAEMA; (b−e) C 1s, O 1s, N 1s, and P 2p core-level high-resolution spectra of PFAA-DOPO-b-PDEAEMA, respectively.

Table 1. Binding Energy and Peak Area of XPS C 1s, O 1s, N 1s and P 2p Peaks of PFAA-DOPO-b-PDEAEMA

Items	Functional group	Peak position, eV	Percentage of area, %
C 1s	(biphenyl)	284.37	17.115
	$-CH_3$ / $-CH_2$ / $-CH-$ / $-C-$	285	44.340
	-C-O- / -C-N- / -C-P-	285.56	31.104
	$-C(=O)-$	288.5	7.441
O 1s	-P-O-	532.3	15.385
	-P=O	531.52	15.385
	-C-O- / (phenyl)-O-	533.2	42.308
	$-C(=O)-$	532	26.922
N 1s	-C-N-	398.88	100.000
P 2p	O=P-O-	132.61	100.000

polystyrene, the HRC, pHRR, and THR of the composites decreased obviously, and when the PFAA-DOPO-*b*-PDEAEMA content was 15 wt %, the HRC, pHRR, and THR of the composites decreased by 44.01%, 37.61%, and 42.89%, respectively, compared with pure polystyrene. In addition, the FRI values of PFAA-DOPO-*b*-PDEAEMA composites are all greater than 1 and less than 10, which shows that the flame retardant performance of PFAA-DOPO-*b*-PDEAEMA is "good". When the mass percentage of PFAA-DOPO-*b*-PDEAEMA is 15 wt %, the flame retardant ability of the

flame retardant in this study is relatively good compared with the flame retardant index of the flame retardant summarized by Vahabi in the literature.[64,70]

3.3. Antistatic Properties of PFAA-DOPO-*b*-PDEAE-MA. Table 3 gives the surface resistivity and volume resistivity of polystyrene composites with addition of 0, 2, 4, 6, 8, 10, and 15 wt % PFAA-DOPO-*b*-PDEAEMA in polystyrene. The data in Table 3 show that the addition of PFAA-DOPO-*b*-PDEEMA can reduce the surface resistivity and volume resistivity of polystyrene composites; when the addition
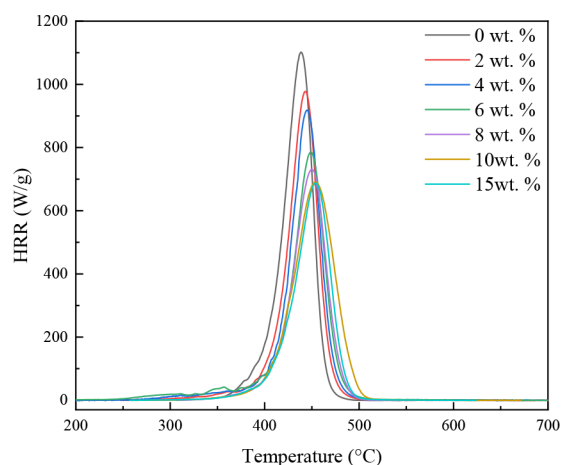
Figure 4. HRR curves of polystyrene composites with PFAA-DOPO-b-PDEAEMA contents of 0, 2, 4, 6, 8, 10, and 15 wt %.

Table 3. Surface Resistivity and Volume Resistivity of Polystyrene Composites with Addition of 0, 2, 4, 6, 8, 10, and 15 wt % PFAA-DOPO-b-PDEAEMA in Polystyrene

content (wt %)	surface resistivity (Ω)	volume resistivity (Ω m)
0	1.68×10^{16}	1.59×10^{15}
2	1.21×10^{16}	9.58×10^{14}
4	4.8×10^{15}	7.66×10^{14}
6	3.6×10^{15}	2.65×10^{14}
8	1.92×10^{15}	1.19×10^{14}
10	7.5×10^{14}	5.4×10^{13}
15	3.3×10^{14}	2.9×10^{13}

amount of PFAA-DOPO-b-PDEEMA is 15 wt %, the surface resistivity and volume resistivity of composites decrease by 2 orders of magnitude. The surface resistivity and volume resistivity of polystyrene composites decreased to 1.96% and 1.82% of the surface resistivity and volume resistivity of pure polystyrene, respectively. It can be seen that the addition of PFAA-DOPO-b-PDEEMA can reduce the surface resistivity and volume resistivity of polystyrene composites to a certain extent, and it is promising as a potential electromagnetic interference shielding material.

4. CONCLUSIONS

A novel bifunctional high-molecular-weight block copolymer based on the DOPO structure was synthesized by the ATRP technique. The addition of PFAA-DOPO-b-PDEAEMA has an obvious influence on the flame retardant properties of PS materials and has a certain degree of influence on the electrical conductivity of PS materials. When the addition of PFAA-DOPO-b-PDEAEMA was 15 wt %, the LOI value of polystyrene increased from 18.5% to 28.4%, the UL-94 test reached V-0 grade, the flame retardant index value reached 2.98, the flame retardant ability was "good", and the volume resistivity and surface resistivity decreased by 2 orders of magnitude. It can be seen that the flame retardant property of PFAA-DOPO-b-PDEAEMA is remarkable, while the antistatic property is slightly improved. In the future, it is necessary to solve the problem of the low antistatic performance of PFAA-DOPO-b-PDEAEMA.

■ AUTHOR INFORMATION

Corresponding Authors

Shaobo Dong − *College of Chemistry and Chemical Engineering, Northeast Petroleum University, Daqing 163318, People's Republic of China; Heilongjiang Province Key Laboratory of Polymeric Composition Material, College of Materials Science and Engineering, Qiqihar University, Qiqihar 161006, People's Republic of China;* orcid.org/0000-0002-9443-3469; Email: dongshaobo1990@163.com

Yazhen Wang − *College of Chemistry and Chemical Engineering, Northeast Petroleum University, Daqing 163318, People's Republic of China; Heilongjiang Province Key Laboratory of Polymeric Composition Material, College of Materials Science and Engineering, Qiqihar University, Qiqihar 161006, People's Republic of China; College of Chemistry, Chemical Engineering and Resource Utilization, Northeast Forestry University, Harbin 150040, People's Republic of China;* Email: wyz6166@nefu.edu.cn

Authors

Tianyu Lan − *College of Chemistry and Chemical Engineering, Northeast Petroleum University, Daqing 163318, People's Republic of China; Heilongjiang Province Key Laboratory of Polymeric Composition Material, College of Materials Science and Engineering, Qiqihar University, Qiqihar 161006, People's Republic of China*

Jianxin Wang − *Heilongjiang Province Key Laboratory of Polymeric Composition Material, College of Materials Science and Engineering, Qiqihar University, Qiqihar 161006, People's Republic of China*

Liwu Zu − *Heilongjiang Province Key Laboratory of Polymeric Composition Material, College of Materials Science and Engineering, Qiqihar University, Qiqihar 161006, People's Republic of China*

Table 2. UL-94, LOI, CC, and FRI of Polystyrene Composites with Addition of 0, 2, 4, 6, 8, 10, and 15 wt % PFAA-DOPO-b-PDEAEMA in Polystyrene[a]

content (wt %)	UL-94	LOI (%)	HRC (J g^{-1} K^{-1})	TT I(s)	pHRR (W g^{-1})	THR (kJ g^{-1})	T_p (°C)	FRI
0	N/A	18.5	1161.0	33.1	1101.6	47.8	438.4	1
2	V-2	19.9	901.8	33.5	977.5	38.3	443.2	1.42
4	V-2	21.3	792.4	34.8	918.0	36.3	445.1	1.66
6	V-1	23.2	720.8	34.8	785.2	28.8	448.7	2.45
8	V-0	23.4	658.3	34.9	730.7	28.4	450.2	2.68
10	V-0	28.1	751.4	35.1	690.6	27.5	453.7	2.94
15	V-0	28.4	650.1	35.1	687.3	27.3	454.1	2.98

[a]Abbreviations: HRC, heat release capacity; pHRR, peak heat release rate; THR, total heat release; T_p, temperature of pHRR.

Tianyuan Xiao − *College of Light Industry and Textile, Qiqihar University, Qiqihar 161006, People's Republic of China*

Yonghui Yang − *Heilongjiang Province Key Laboratory of Polymeric Composition Material, College of Materials Science and Engineering, Qiqihar University, Qiqihar 161006, People's Republic of China*

Jun Wang − *College of Chemistry and Chemical Engineering, Northeast Petroleum University, Daqing 163318, People's Republic of China*

Complete contact information is available at:
https://pubs.acs.org/10.1021/acsomega.2c05809

Author Contributions

S.D. and Y.W. contributed equally to this work.

Notes

The authors declare no competing financial interest.

■ REFERENCES

(1) Vahabi, H.; Laoutid, F.; Mehrpouya, M.; Saeb, M. R.; Dubois, P. Flame retardant polymer materials: An update and the future for 3D printing developments. *Mater. Sci. Eng., R* **2021**, *144*, 100604.

(2) Vahabi, H.; Laoutid, F.; Formela, K.; Saeb, M. R.; Dubois, P. Flame-retardant polymer materials developed by reactive extrusion: present status and future perspectives. *Polym. Rev.* **2022**, *62*, 919.

(3) Zhou, H.; Wen, D.; Hao, X.; Chen, C.; Zhao, N.; Ou, R.; Wang, Q. Nanostructured multifunctional wood hybrids fabricated via in situ mineralization of zinc borate in hierarchical wood structures. *Chem. Eng. J.* **2023**, *451*, 138308.

(4) Zhu, G.; Li, H.; Deng, S.; Zhang, C.; Kang, K. A multifunctional ZnO-ZIF-8/bamboo composite with enhanced adsorption capacity and improved flame retardancy. *Wood Mater. Sci. Eng.* **2022**, 1.

(5) Zhu, D.; Bi, Q.; Yin, G.; Jiang, Y.; Fu, W.; Wang, N.; Wang, D. Investigation of magnesium hydroxide functionalized by polydopamine/transition metal ions on flame retardancy of epoxy resin. *J. Therm. Anal. Calorim.* **2022**, DOI: 10.1007/s10973-022-11467-5.

(6) Zhou, L.; Li, W.; Zhao, H.; Wang, J.; Zhao, B. NiTi-layered double hydroxide nanosheets toward high-efficiency flame retardancy and smoke suppression for silicone foam. *Polym. Degrad. Stab.* **2022**, *204*, 110104.

(7) Liu, Y.; Yu, Z.; Lu, G.; Chen, W.; Ye, Z.; He, Y.; Tang, Z.; Zhu, J. Versatile levulinic acid-derived dynamic covalent thermosets enabled by in situ generated imine and multiple hydrogen bonds. *Chem. Eng. J.* **2023**, *451*, 139053.

(8) Zhu, Y.; Wu, W.; Xu, T.; Xu, H.; Zhong, Y.; Zhang, L.; Ma, Y.; Sui, X.; Wang, B.; Feng, X.; Mao, Z. Effect of weak intermolecular interactions in micro/nanoscale polyphosphazenes and polyethylene terephthalate composites on flame retardancy. *Polym. Adv. Technol.* **2022**, *33*, 2231.

(9) Zhu, Y.; Wu, W.; Xu, T.; Xu, H.; Zhong, Y.; Zhang, L.; Ma, Y.; Sui, X.; Wang, B.; Feng, X.; Mao, Z. Preparation and characterization of polyphosphazene-based flame retardants with different functional groups. *Polym. Degrad. Stab.* **2022**, *196*, 109815.

(10) Zhou, X.; Yu, R.; Jiang, J.; Dang, J.; Luan, J.; Wang, G.; Zhang, M. PEEK composite resin with enhanced intumescent flame retardancy loaded with Octaphenylsilsesquioxane and nano calcium carbonate and its application in fibers. *Polym. Degrad. Stab.* **2022**, *202*, 110042.

(11) Zhang, W.; Huang, J.; Guo, X.; Zhang, W.; Qian, L.; Qin, Z. Double organic groups-containing polyhedral oligomeric silsesquioxane filled epoxy with enhanced fire safety. *J. Appl. Polym. Sci.* **2022**, DOI: 10.1002/app.52461.

(12) Lyu, B.; Kou, M.; Gao, D.; Luo, K.; Ma, J.; Lin, Y. Flame retardancy of carboxylated polyhedral oligosilsesquioxane modified layered double hydroxide in the process of leather fatliquoring. *J. Appl. Polym. Sci.* **2022**, DOI: 10.1002/app.52468.

(13) Rad, E. R.; Vahabi, H.; de Anda, A. R.; Saeb, M. R.; Thomas, S. Bio-epoxy resins with inherent flame retardancy. *Prog. Org. Coat.* **2019**, *135*, 608−612.

(14) Solihat, N. N.; Hidayat, A. F.; Taib, M. N. A. M.; Hussin, M. H.; Lee, S. H.; Ghani, M. A. A.; Edrus, S. S. O. A.; Vahabi, H.; Fatriasari, W. Recent developments in flame-retardant lignin-based biocomposite: manufacturing, and characterization. *J. Polym. Environ.* **2022**.

(15) Li, X.; Shi, X.; Chen, M.; Liu, Q.; Li, Y.; Li, Z.; Huang, Y.; Wang, D. Biomass-based coating from chitosan for cotton fabric with excellent flame retardancy and improved durability. *Cellulose* **2022**, *29*, 5289.

(16) Li, C.; Wang, B.; Zhou, L.; Hou, X.; Su, S. Effects of ligninbased flame retardants on flame-retardancy and insulation performances of epoxy resin composites. *Iran. Polym. J.* **2022**, *31*, 949.

(17) Xu, J.; Niu, Y.; Xie, Z.; Liang, F.; Guo, F.; Wu, J. Synergistic flame retardant effect of carbon nanohorns and ammonium polyphosphate as a novel flame retardant system for cotton fabrics. *Chem. Eng. J.* **2023**, *451*, 138566.

(18) Jiang, G.; Xiao, Y.; Qian, Z.; Yang, Y.; Jia, P.; Song, L.; Hu, Y.; Ma, C.; Gui, Z. A novel phosphorus-, nitrogen- and sulfur-containing macromolecule flame retardant for constructing high-performance epoxy resin composites. *Chem. Eng. J.* **2023**, *451*, 137823.

(19) Zhu, Y.; Cai, W.; Zhao, Y.; Mu, X.; Zhou, X.; Chu, F.; Wang, B.; Hu, Y. Graphite-like carbon nitride/polyphosphoramide nanohybrids for enhancement on thermal stability and flame retardancy of thermoplastic polyurethane elastomers. *ACS Appl. Polym. Mater.* **2022**, *4*, 121.

(20) Zhou, W.; Lv, D.; Ding, H.; Xu, P.; Zhang, C.; Ren, Y.; Yang, W.; Ma, P. Synthesis of eugenol-based phosphorus-containing epoxy for enhancing the flame-retardancy and mechanical performance of DGEBA epoxy resin. *React. Funct. Polym.* **2022**, *180*, 105383.

(21) Tan, W.; Ren, Y.; Guo, Y.; Liu, Y.; Liu, X.; Qu, H. A novel multi-claw reactive flame retardant derived from DOPO for endowing lyocell fabric with high effective flame retardancy. *Cellulose* **2022**, *29*, 6941.

(22) Ma, L.; Liu, H.; Wen, X.; Szymańska, K.; Mijowska, E.; Hao, C.; Tang, T.; Lei, Q. Polyhydric SiO_2 coating assistant to graft organophosphorus onto glass fabric for simultaneously improving flame retardancy and mechanical properties of epoxy resin composites. *Composites, Part B* **2022**, *243*, 110176.

(23) Liu, D.; Zhao, W.; Cui, Y.; Zhang, T.; Ji, P. Influence of the chemical structure on the flame retardant mechanism and mechanical properties of flame-retardant epoxy resin thermosets. *Macromol. Mater. Eng.* **2022**, *307*, 2200169.

(24) Zhao, Z.; Tan, Y.; Guo, S.; Ni, X. An efficient composite modifier prepared for enhancing the crystallization and flame-retardancy of poly(m-xylylene adipamide). *Polymers* **2022**, *14* (17), 3626.

(25) Zhao, W.; Wang, J.; Zhuang, G.; Liu, D.; Sun, C. Thermal stability and flame retardancy of epoxy resin with DOPO-based compound containing triazole and hydroxyl groups. *Macromol. Mater. Eng.* **2022**, *307*, 2200408.

(26) Zhang, D.; Shang, X.; Luo, J.; Sun, J.; Tan, F.; Bao, D.; Qin, S. Flame retardancy properties and rheological behavior of PP/DiDOPO conjugated flame retardant composites. *Front. Chem.* **2022**, *10*, 933716.

(27) Yang, Y.; Chen, W.; Li, Z.; Huang, G.; Wu, G. Efficient flame retardancy, good thermal stability, mechanical enhancement, and transparency of DOPO-conjugated structure compound on epoxy resin. *Chem. Eng. J.* **2022**, *450*, 138424.

(28) Chen, P.; Wu, Z.; Guo, T.; Zhou, Y.; Liu, M.; Xia, X.; Sun, J.; Lu, L.; Ouyang, X.; Wang, X.; Fu, Y.; Zhu, J. Strong chemical interaction between lithium polysulfides and flame-retardant polyphosphazene for lithium-sulfur batteries with enhanced safety and electrochemical performance. *Adv. Mater.* **2021**, *33*, 2007549.

(29) Chu, F.; Xu, Z.; Zhou, Y.; Zhang, S.; Mu, X.; Wang, J.; Hu, W.; Song, L. Hierarchical core−shell TiO_2@LDH@Ni(OH)$_2$ architecture with regularly-oriented nanocatalyst shells: Towards improving the mechanical performance, flame retardancy and toxic smoke suppression of unsaturated polyester resin. *Chem. Eng. J.* **2021**, *405*, 126650.

(30) Han, G.; Zhao, X.; Feng, Y.; Ma, J.; Zhou, K.; Shi, Y.; Liu, C.; Xie, X. Highly flame-retardant epoxy-based thermal conductive composites with functionalized boron nitride nanosheets exfoliated by one-step ball milling. *Chem. Eng. J.* **2021**, *407*, 127099.

(31) He, G.; Wang, L.; Bao, X.; Lei, Z.; Ning, F.; Li, M.; Zhang, X.; Qu, L. Synergistic flame retardant weft-knitted alginate/viscose fabrics with MXene coating for multifunctional wearable heaters. *Composites, Part B* **2022**, *232*, 109618.

(32) Huang, G.; Chen, W.; Wu, T.; Guo, H.; Fu, C.; Xue, Y.; Wang, K.; Song, P. Multifunctional graphene-based nano-additives toward high-performance polymer nanocomposites with enhanced mechanical, thermal, flame retardancy and smoke suppressive properties. *Chem. Eng. J.* **2021**, *410*, 127590.

(33) Liu, L.; Xu, Y.; Pan, Y.; Xu, M.; Di, Y.; Li, B. Facile synthesis of an efficient phosphonamide flame retardant for simultaneous enhancement of fire safety and crystallization rate of poly (lactic acid). *Chem. Eng. J.* **2021**, *421*, 127761.

(34) Liu, L.; Zhu, M.; Ma, Z.; Xu, X.; Mohesen Seraji, S.; Yu, B.; Sun, Z.; Wang, H.; Song, P. A reactive copper-organophosphate-MXene heterostructure enabled antibacterial, self-extinguishing and mechanically robust polymer nanocomposites. *Chem. Eng. J.* **2022**, *430*, 132712.

(35) Qi, F.; Wang, L.; Zhang, Y.; Ma, Z.; Qiu, H.; Gu, J. Robust $Ti_3C_2T_x$ MXene/starch derived carbon foam composites for superior EMI shielding and thermal insulation. *Mater. Today Phys.* **2021**, *21*, 100512.

(36) Wang, L.; Ma, Z.; Zhang, Y.; Qiu, H.; Ruan, K.; Gu, J. Mechanically strong and folding-endurance $Ti_3C_2T_x$ MXene/PBO nanofiber films for efficient electromagnetic interference shielding and thermal management. *Carbon Energy* **2022**, *4*, 200.

(37) Xiang, J.; Zhang, Y.; Zhang, B.; Yuan, L.; Liu, X.; Cheng, Z.; Yang, Y.; Zhang, X.; Li, Z.; Shen, Y.; Jiang, J.; Huang, Y. A flame-retardant polymer electrolyte for high performance lithium metal batteries with an expanded operation temperature. *Energy Environ. Sci.* **2021**, *14*, 3510.

(38) Xiang, Z.; Wang, X.; Zhang, X.; Shi, Y.; Cai, L.; Zhu, X.; Dong, Y.; Lu, W. Self-assembly of nano/microstructured 2D Ti_3CNT_x MXene-based composites for electromagnetic pollution elimination and Joule energy conversion application. *Carbon* **2022**, *189*, 305−318.

(39) Yang, H.; Shi, B.; Xue, Y.; Ma, Z.; Liu, L.; Liu, L.; Yu, Y.; Zhang, Z.; Annamalai, P. K.; Song, P. Molecularly engineered lignin-derived additives enable fire-retardant, uv-shielding, and mechanically strong polylactide biocomposites. *Biomacromolecules* **2021**, *22*, 1432.

(40) Yu, B.; Yuen, A. C. Y.; Xu, X.; Zhang, Z.; Yang, W.; Lu, H.; Fei, B.; Yeoh, G. H.; Song, P.; Wang, H. Engineering MXene surface with POSS for reducing fire hazards of polystyrene with enhanced thermal stability. *J. Hazard. Mater.* **2021**, *401*, 123342.

(41) Zhang, X.; Liu, Z.; Deng, B.; Cai, L.; Dong, Y.; Zhu, X.; Lu, W. Honeycomb-like $NiCo_2O_4$@MnO_2 nanosheets array/3D porous expanded graphite hybrids for high-performance microwave absorber with hydrophobic and flame-retardant functions. *Chem. Eng. J.* **2021**, *419*, 129547.

(42) Zhang, Y.; Jing, J.; Liu, T.; Xi, L.; Sai, T.; Ran, S.; Fang, Z.; Huo, S.; Song, P. A molecularly engineered bioderived polyphosphate for enhanced flame retardant, UV-blocking and mechanical properties of poly(lactic acid). *Chem. Eng. J.* **2021**, *411*, 128493.

(43) Gao, C.; Shi, Y.; Zhu, S.; Fu, L.; Feng, Y.; Lv, Y.; Yang, F.; Liu, M.; Shui, W. Induced assembly of polystyrene composites for simultaneously improving flame retardant and electromagnetic shielding properties. *Polym. Adv. Technol.* **2021**, *32*, 4251.

(44) Lee, S.; Hong, Y.; Shim, B. S. Biodegradable PEDOT:PSS/clay composites for multifunctional green-electronic materials. *Adv. Sustainable Syst.* **2022**, *6*, 2100056.

(45) Sakhadeo, N. N.; Patro, T. U. Exploring the multifunctional applications of surface-coated polymeric foams—a review. *Ind. Eng. Chem. Res.* **2022**, *61* (16), 5366−5387.

(46) Gao, C.; Shi, Y.; Chen, Y.; Zhu, S.; Feng, Y.; Lv, Y.; Yang, F.; Liu, M.; Shui, W. Constructing segregated polystyrene composites for excellent fire resistance and electromagnetic wave shielding. *J. Colloid Interface Sci.* **2022**, *606*, 1193.

(47) Gao, C.; Shi, Y.; Huang, R.; Feng, Y.; Chen, Y.; Zhu, S.; Lv, Y.; Shui, W.; Chen, Z. Creating multilayer-structured polystyrene composites for enhanced fire safety and electromagnetic shielding. *Composites, Part B* **2022**, *242*, 110068.

(48) Li, L.; Shao, X.; Zhao, Z.; Liu, X.; Jiang, L.; Huang, K.; Zhao, S. Synergistic fire hazard effect of a multifunctional flame retardant in building insulation expandable polystyrene through a simple surface-coating method. *ACS Omega* **2020**, *5* (1), 799−807.

(49) Yuan, B.; Zhao, H.; Yang, F.; Zhang, J.; Wu, Y.; Qi, C.; Tan, Z.; Zhang, G.; Ren, B.; Xiao, F. The design of a metal−organic framework with flame-retardant performance and bionic hydrophobic surface inspired by the lotus leaf. *New J. Chem.* **2022**, *46*, 17874.

(50) Zhu, S. e.; Yang, W.; Zhou, Y.; Pan, W.; Wei, C.; Yuen, A. C. Y.; Chen, T. B. Y.; Yeoh, G. H.; Lu, H.; Yang, W. Synthesis of zinc porphyrin complex for improving mechanical, UV-resistance, thermal stability and fire safety properties of polystyrene. *Chem. Eng. J.* **2022**, *442*, 136367.

(51) Masuda, T.; Takai, M. Design of biointerfaces composed of soft materials using controlled radical polymerizations. *J. Mater. Chem. B* **2022**, *10*, 1473.

(52) Cao, M.; Liu, Y.; Zhang, X.; Li, F.; Zhong, M. Expanding the toolbox of controlled/living branching radical polymerization through simulation-informed reaction design. *Chem.* **2022**, *8* (5), 1460−1475.

(53) Zhao, B. Shape-changing bottlebrush polymers. *J. Phys. Chem. B* **2021**, *125*, 6373.

(54) Tong, Y.; Liu, Y.; Chen, Q.; Mo, Y.; Ma, Y. Long-lived triplet excited-state bichromophoric iridium photocatalysts for controlled photo-mediated atom-transfer radical polymerization. *Macromolecules* **2021**, *54*, 6117.

(55) Raffa, P.; Kassi, A.; Gosschalk, J.; Migliore, N.; Polgar, L. M.; Picchioni, F. A structure-properties relationship study of self-healing materials based on styrene and furfuryl methacrylate cross-linked via diels−alder chemistry. *Macromol. Mater. Eng.* **2021**, *306*, 2000755.

(56) Kaupbayeva, B.; Boye, S.; Munasinghe, A.; Murata, H.; Matyjaszewski, K.; Lederer, A.; Colina, C. M.; Russell, A. J. Molecular dynamics-guided design of a functional protein-atrp conjugate that eliminates protein-protein interactions. *Bioconjugate Chem.* **2021**, *32*, 821.

(57) Feiz, E.; Mahyari, M.; Ghaieni, H. R.; Tavangar, S. Copper on chitosan-modified cellulose filter paper as an efficient dip catalyst for ATRP of MMA. *Sci. Rep.* **2021**, *11* (1), 8257.

(58) Celentano, W.; Ordanini, S.; Bruni, R.; Marocco, L.; Medaglia, P.; Rossi, A.; Buzzaccaro, S.; Cellesi, F. Complex poly(ε-caprolactone)/poly(ethylene glycol) copolymer architectures and their effects on nanoparticle self-assembly and drug nanoencapsulation. *Eur. Polym. J.* **2021**, *144*, 110226.

(59) Cao, M.; Zhong, M. Chain-growth branching radical polymerization: an inibramer strategy. *Polym. Int.* **2022**, *71*, 501.

(60) Tamura, M.; Kurokawa, N.; Hotta, A. Compensation for orientation birefringence of PMMA by blending bottlebrush polymers composed of well-controlled graft chains. *ACS Macro Lett.* **2022**, *11* (6), 799−804.

(61) Cao, Y.; Wang, X.; Zhang, W.; Yin, X.; Shi, Y.; Wang, Y. Bi-DOPO structure flame retardants with or without reactive group: their effects on thermal stability and flammability of unsaturated polyester. *Ind. Eng. Chem. Res.* **2017**, *56* (20), 5913−5924.

(62) Constantinou, A. P.; Lan, T.; Carroll, D. R.; Georgiou, T. K. Tricomponent thermoresponsive polymers based on an amine-containing monomer with tuneable hydrophobicity: Effect of composition. *Eur. Polym. J.* **2020**, *130*, 109655.

(63) Fang, Y.; Zhou, X.; Xing, Z.; Wu, Y. An effective flame retardant for poly(ethylene terephthalate) synthesized by phospha-phenanthrene and cyclotriphosphazene. *J. Appl. Polym. Sci.* **2017**, *134* (35), 45246.

(64) Vahabi, H.; Kandola, B. K.; Saeb, M. R. Flame retardancy index for thermoplastic composites. *Polymers* **2019**, *11* (3), 407.

(65) Vahabi, H.; Laoutid, F.; Movahedifar, E.; Khalili, R.; Rahmati, N.; Vagner, C.; Cochez, M.; Brison, L.; Ducos, F.; Ganjali, M. R.; Saeb, M. R. Description of complementary actions of mineral and organic additives in thermoplastic polymer composites by Flame Retardancy Index. *Polym. Adv. Technol.* **2019**, *30* (8), 2056−2066.

(66) Quan, Y.; Zhang, Z.; Tanchak, R. N.; Wang, Q. A review on cone calorimeter for assessment of flame-retarded polymer composites. *J. Therm. Anal. Calorim.* **2022**, *147*, 10209.

(67) Dong, Q.*Infrared Spectroscopy*; Petrochemical Industry Press: 1977; pp 1−304.

(68) Lu, Y.; Deng, Z.*Practical infrared spectrum analysis*; Electronic Industry Press: 1989; pp 1−278.

(69) Beamson, G.; Briggs, D.*High Resolution XPS of Organic Polymers−The Scienta ESCA300 Database*; Wiley: 1992; pp 1−295.

(70) Movahedifar, E.; Vahabi, H.; Saeb, M. R.; Thomas, S. Flame Retardant Epoxy Composites on the Road of Innovation: An Analysis with Flame Retardancy Index for Future Development. *Molecules* **2019**, *24* (21), 3964.